Neurulation and neurite extension require the zinc transporter ZIP12 (*slc39a12*)

Winyoo Chowanadisai[a,b,1], David M. Graham[c], Carl L. Keen[a], Robert B. Rucker[a], and Mark A. Messerli[b,c]

[a]Department of Nutrition, University of California, Davis, CA 95616; [b]Cellular Dynamics Program, Marine Biological Laboratory, Woods Hole, MA 02543; and [c]Eugene Bell Center for Regenerative Biology and Tissue Engineering, Marine Biological Laboratory, Woods Hole, MA 02543

Edited by Yuh Nung Jan, Howard Hughes Medical Institute, University of California San Francisco, San Francisco, CA, and approved May 1, 2013 (received for review December 19, 2012)

Zn^{2+} is required for many aspects of neuronal structure and function. However, the regulation of Zn^{2+} in the nervous system remains poorly understood. Systematic analysis of tissue-profiling microarray data showed that the zinc transporter ZIP12 (*slc39a12*) is highly expressed in the human brain. In the work reported here, we confirmed that ZIP12 is a Zn^{2+} uptake transporter with a conserved pattern of high expression in the mouse and *Xenopus* nervous system. Mouse neurons and Neuro-2a cells produce fewer and shorter neurites after ZIP12 knockdown without affecting cell viability. Zn^{2+} chelation or loading in cells to alter Zn^{2+} availability respectively mimicked or reduced the effects of ZIP12 knockdown on neurite outgrowth. ZIP12 knockdown reduces cAMP response element-binding protein activation and phosphorylation at serine 133, which is a critical pathway for neuronal differentiation. Constitutive cAMP response element-binding protein activation restores impairments in neurite outgrowth caused by Zn^{2+} chelation or ZIP12 knockdown. ZIP12 knockdown also reduces tubulin polymerization and increases sensitivity to nocodazole following neurite outgrowth. We find that ZIP12 is expressed during neurulation and early nervous system development in *Xenopus tropicalis,* where ZIP12 antisense morpholino knockdown impairs neural tube closure and arrests development during neurulation with concomitant reduction in tubulin polymerization in the neural plate. This study identifies a Zn^{2+} transporter that is specifically required for nervous system development and provides tangible links between Zn^{2+}, neurulation, and neuronal differentiation.

brain development | CREB | neural tube defect | zinc deficiency | birth defects

Approximately 12% of Americans fail to consume the Estimated Average Requirement for Zn^{2+} and could be at risk for zinc deficiency (1). Zn^{2+} is a nutrient that plays critical roles in more than 1,000 proteins, including enzyme catalysis, cell signaling, and DNA repair (2), and as a result is essential for neural development, learning, and memory (3). Gene–nutrient interactions influence brain development, structure, and function throughout all stages of life (4). Zn^{2+} supplementation can reduce the risk for certain pregnancy complications (5–7), including congenital defects, by preventing primary deficiencies caused by diet or by treating secondary deficiencies, such as acrodermatitis enteropathica, a genetic disorder caused by a defect in intestinal Zn^{2+} transport secondary to a mutation in the Zn^{2+} IRT-like protein ZIP4 (5). Members of the solute carrier 39 (SLC39) gene family encoding the Zn^{2+} IRT-like proteins (ZIPs) are important components of cellular Zn^{2+} homeostasis and encode proteins that promote cellular Zn^{2+} uptake in a wide range of species (8). In vertebrates, mutations in some SLC39 members have been linked to developmental and metabolic disorders (5, 9–13), generally leading to pleiotropic phenotypes.

Here, we analyzed published genome-wide microarray data (14) to determine that *slc39a12* (ZIP12) is highly expressed in the human brain relative to other SLC30 and SLC39 transporters. We used a reverse genetics approach to demonstrate that ZIP12 is an essential Zn^{2+} transporter predominantly expressed in the brain. We observed that ZIP12 is important for multiple aspects of neuronal differentiation, including activation of cAMP response element-binding protein (CREB), tubulin polymerization, and neurite extension, in vitro. We show that ZIP12 is required for neurulation and embryonic viability during *Xenopus tropicalis* development. These findings show that the Zn^{2+} transporter ZIP12 represents a point of regulation that links Zn^{2+} directly to nervous system development.

Results

ZIP12 Is Highly Expressed in the Brain. We analyzed a previously published microarray dataset (14) for human genes in the SLC30 and SLC39 families with brain-specific patterns of expression that are likely to be important for nervous system development and function (Fig. S1*A*). Of 32,878 probe sets, 1,130 genes (3.44%) had a brain expression ratio greater than 5; of these, 1,118 genes (3.40%) were annotated with a gene symbol, National Center for Biotechnology Information accession number, or Celera transcript number (Dataset S1). The gene expression of *slc39a12* is 47-fold higher in the human brain than in other tissues (Fig. S1*A*). The top five genes with the highest brain-expression ratios (Dataset S1) have documented nervous system-specific expression patterns and functions. The high expression of ZIP12 in the human brain identified in our analysis is consistent with a previous transcriptome analysis using expressed sequence tag data (8).

Next, we examined *slc39a12* expression in mice to gain insight into the possible physiological roles of ZIP12. Our gene-expression analysis revealed high levels of mZIP12 mRNA in brain (Fig. 1*A*). We created an mZIP12-specific antibody that binds to an N-terminal epitope before the first transmembrane domain (Fig. 1*B*). mZIP12 protein expression was primarily in the mouse brain (Fig. 1*C*) and was detected in the hippocampus, frontal cortex, striatum, hypothalamus, and cerebellum (Fig. 1*D*). Primary mouse neurons have endogenous ZIP12 expression at the plasma membrane (Fig. 1*E*). mZIP12 localization to the plasma membrane also was confirmed via epitope labeling in unpermeabilized CHO cells transfected with mZIP12-HA (Fig. S1 *B–E*). Sequestration of extracellular Zn^{2+} with the Zn^{2+} chelator N,N,N′,N′-tetrakis(2-pyridylmethyl)ethylenediamine (TPEN) resulted in a redistribution of mZIP12 from the perinuclear space to the cytoplasm and plasma membrane, as detected by indirect immunofluorescence (Fig. S1*D*) and cell-surface protein biotinylation (Fig. S1*E*). TPEN also increased Zn^{2+} uptake in both control and mZIP12-transfected cells (Fig. S1*F*), indicating that mZIP12 is present at the plasma membrane of transfected CHO cells.

Author contributions: W.C., D.M.G., R.B.R., and M.A.M. designed research; W.C., D.M.G., and M.A.M. performed research; C.L.K. contributed new reagents/analytic tools; W.C., D.M.G., and M.A.M. analyzed data; and W.C., D.M.G., C.L.K., R.B.R., and M.A.M. wrote the paper.

The authors declare no conflict of interest.

This article is a PNAS Direct Submission.

[1]To whom correspondence should be addressed. E-mail: wchowanadisai@ucdavis.edu.

This article contains supporting information online at www.pnas.org/lookup/suppl/doi:10.1073/pnas.1222142110/-/DCSupplemental.

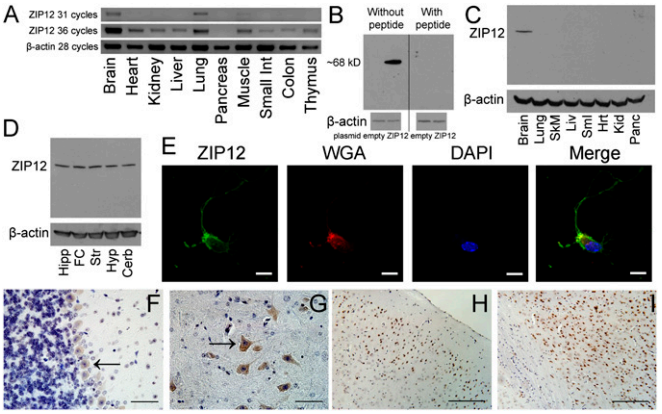

Fig. 1. ZIP12 is primarily expressed in the human and mouse brain. (*A*) ZIP12 mRNA expression detected in various mouse tissues by RT-PCR. (*B*) Detection of mouse ZIP12 by immunoblotting in mZIP12-transfected CHO cells. (*C* and *D*) ZIP12 protein expression detected in various mouse tissue lysates (*C*) and brain region lysates (*D*) by immunoblotting. (*C*) Tissues include (from left to right): brain, lung, skeletal muscle, liver, small intestine, heart, kidney, and pancreas. (*D*) Brain regions include (from left to right): hippocampus (Hipp), frontal cortex (FC), striatum (Str), hypothalamus (Hyp), and cerebellum (Cerb). (*E*) ZIP12 is present at the plasma membrane in primary mouse neurons. (Scale bar: 10 μm.) (*F–I*) ZIP12 is present in coronal sections of various regions of the mouse brain. Brain regions include (*F*) cerebellum (including Purkinje cell layer), (*G*) medulla oblongata, (*H*) frontal cortex, and (*I*) corpus callosum (and cortex). Arrows in *F* and *G* indicate neuronal staining. [Scale bar: 50 μm (60× magnification) in *F* and *G*; 200 μm (20× magnification) in *H* and *I*.]

mZIP12 protein also was detected in neurons in the Purkinje cell layer of the cerebellum (Fig. 1*F*), medulla oblongata (Fig. 1*G*), and the frontal cortex (Fig. 1 *H* and *I*). No staining was detected in the granule cells of the cerebellum (Fig. 1*F*), indicating that not all neurons express ZIP12. The high expression of ZIP12 in the brain suggests a functional role for ZIP12-mediated Zn^{2+} transport in the nervous system.

***slc39a12* Encodes the Zn^{2+} Transporter, ZIP12.** The gene *slc39a12* encodes a putative member of the SLC39 gene family of Zn^{2+} transporters. We characterized the kinetic properties of mZIP12 by transfecting CHO cells and measuring Zn^{2+} uptake using the radioisotope ^{65}Zn in varying concentrations of free Zn^{2+} (Fig. 2). Zn^{2+} uptake was twofold higher in mZIP12-transfected cells than in control cells (Fig. 2*A*). Addition of other metals in excess did not prevent Zn^{2+} uptake (Fig. 2*B*), although copper and cadmium did suppress Zn^{2+} uptake to a slight degree. Excess cold (unlabeled) Zn^{2+} significantly reduced ^{65}Zn uptake in both control and mZIP12-transfected cells. ZIP12 activity is temperature dependent because we did not observe significant Zn^{2+} uptake at 4 °C. We estimated the K_m of mZIP12 to be 6.6 nM, which indicates that mZIP12 has a high affinity for Zn^{2+}, and a V_{max} of 2.7 pmol $Zn^{2+}{\cdot}min^{-1}{\cdot}mg\ protein^{-1}$. Using inductively coupled plasma mass spectrometry (ICP-MS), we observed that mZIP12 induces the accumulation of Zn^{2+} (Fig. 2*C*). Overexpression of ZIP12 increases metal response element (MRE) activation by metal-regulatory transcription factor 1 (MTF-1), a sensitive measure of cytoplasmic Zn^{2+} concentrations (Fig. 2*D*) (15). Zinc sequestration with TPEN also increased Zn^{2+} uptake in both control and mZIP12-transfected cells (Fig. S1*F*). The increase in Zn^{2+} transport by transfection with ZIP12 did not affect cell viability (Fig. 2*E*). These results indicate that increased ZIP12 expression results in higher cellular Zn^{2+} uptake, increased cellular Zn^{2+} accumulation, and increased cytoplasmic Zn^{2+} concentration, consistent with ZIP12 functioning as a Zn^{2+} transporter.

ZIP12 Expression and Intracellular Zn^{2+} Increase During Stimulated Neurite Outgrowth. We conducted studies to determine if neuronal differentiation is accompanied by changes in cellular Zn^{2+} homeostasis and mZIP12 expression. We used the mouse neuroblastoma cell line, Neuro2a (N2a), a well-characterized model for retinoic acid (RA)-induced differentiation (16). Quantitative transcript analysis of endogenous mZIP12 in N2a cells revealed an approximately threefold increase in mZIP12 gene expression in differentiated cells versus control and reduced serum conditions (Fig. S2*A*). A similar increase in mZIP12 mRNA expression was found in neuronal precursor cells (NPCs) (Fig. S2*B*) following differentiation. Endogenous mZIP12 protein expression increased in N2a cells after differentiation (Fig. S2*C*). After 48 h differentiated N2a cells displayed significantly increased Zn^{2+} uptake (Fig. S2*D*), as measured by ^{65}Zn, and increased fluorescence of the zinc fluorophore Zinpyr-1 in perinuclear compartments, as measured by microscopy (Fig. S2*E*) and flow cytometry (Fig. S2 *F* and *G*), compared with undifferentiated cells. Time-dependent increases in neurite extension, an early morphological sign of neuronal differentiation, were observed in N2a cells treated with RA (Fig. S2*H*). These changes in Zn^{2+} metabolism induced by differentiation occurred without affecting cell viability (Fig. S2*I*).

ZIP12 Knockdown Reduces Zn^{2+} Uptake and Neurite Extension During Differentiation. We used a ZIP12-specific shRNA plasmid to knock down expression of endogenous mZIP12 in N2a cells. ZIP12 shRNA effectively reduced mZIP12 mRNA (Fig. S3*A*) and protein (Fig. S3*B*) expression in differentiated N2a cells. Differentiation of N2a cells increased Zn^{2+} uptake, which was decreased by ZIP12-shRNA knockdown (Fig. S3*C*). No difference in cell viability was observed between control cells and N2a cells transfected with ZIP12-shRNA at 48 or 96 h posttransfection (Fig. S3*D*).

In differentiated N2a cells, knockdown of mZIP12 expression resulted in fewer and shorter neurites compared with control

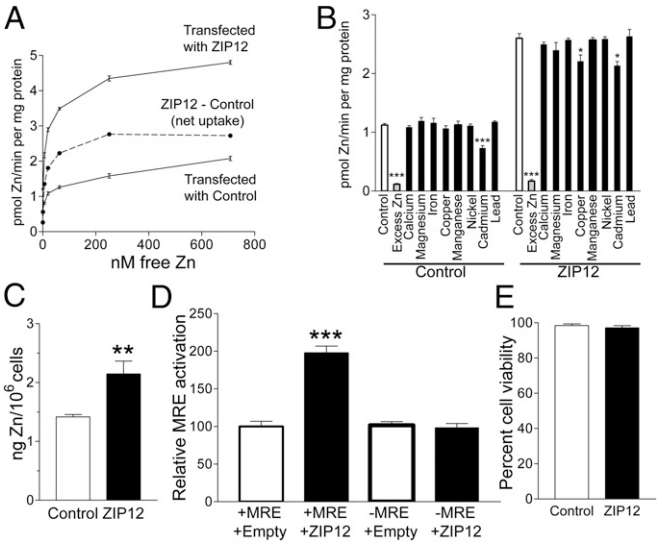

Fig. 2. ZIP12 is a high-affinity, Zn^{2+}- specific transporter. (*A*) Zn^{2+} uptake at different concentrations of free external Zn^{2+} by ZIP12 in CHO cells was measured using ^{65}Zn ($n = 3$, ± SE). The curve marked ZIP12 – Control represents net Zn^{2+} uptake in ZIP12-transfected cells minus uptake in control-transfected cells. (*B*) Zn^{2+} uptake specificity of ZIP12 relative to other metals determined using ^{65}Zn ($n = 3$, ± SE). Excess Zn^{2+} indicates cold Zn^{2+} added to uptake buffer during assay. (*C*) Increased Zn^{2+} content relative to cell number by ZIP12 was measured by ICP-MS ($n = 6$, ± SE). (*D*) ZIP12 increases MRE activation, measured by reporter assay ($n = 6$, ± SE). (*E*) ZIP12 overexpression does not affect cell viability at 48 h posttransfection, measured by Trypan blue exclusion ($n = 6$, ± SE). $^{**}P < 0.01$; $^{***}P < 0.001$ versus control cells.

cells (Table S1). Exposure to RA for periods of 48, 72, and 96 h caused consistently longer neurites in cells treated with control shRNA than in cells treated with ZIP12-shRNA over the same time periods (Fig. 3 *A* and *B* and Fig. S4 *A*–*C*). We observed a decrease in neurite length when N2a cells were differentiated with dibutyryl cAMP instead of RA (Fig. S4*D*). Primary neurons, either directly dissociated from mouse embryonic brain cortices (Fig. S4 *E* and *F*) or primary mouse NPCs (Fig. S4 *G* and *H*), had shorter neurites after 48 h of transfection with ZIP12 shRNA. These observations show that the ZIP12-dependent aberrant neurite phenotype is consistent across many neuronal models of differentiation and is not limited to a specific cell line or dependent on cell line immortalization or specific inducers of differentiation. These data indicate that neurite sprouting and length are linked to intracellular Zn^{2+} and ZIP12 expression.

We characterized the role of Zn^{2+} on neurite outgrowth by manipulating mZIP12 expression with ZIP12-shRNA and availability of extracellular and intracellular Zn^{2+} with the nonpermeant Zn^{2+} chelator diethylene triamine pentaacetic acid (DTPA) and the Zn^{2+} carrier, pyrithione (17), respectively. All experiments reported here were performed on both N2a cells and primary mouse NPCs differentiated for 48 h. Treatment of N2a cells with DTPA resulted in fewer cells expressing neurites (Table S1). DTPA treatment, which reduced available free Zn^{2+} concentrations below detection (Fig. S5 *A* and *B*) in both N2a cells (Fig. 3*C*) and differentiated mouse NPCs (Fig. S4*I*), reduced neurite length in the cells transfected with control shRNA. This phenotype was restored by saturating DTPA with additional Zn^{2+} (Fig. 3*C* and Fig. S4*I*). In comparison, ZIP12 knockdown resulted in cells with fewer neurites (Table S1) and reduced neurite length (Fig. 3*C* and Fig. S4*I*) compared with control cells without DTPA treatment. Treatment of ZIP12-knockdown cells with DTPA alone or Zn^{2+}-saturated DTPA did not have further negative effects on neurite outgrowth. Similar results were found with Zn^{2+}-deficient, Chelex-treated medium. The effects of ZIP12 were observed in N2a cells and differentiated mouse NPCs treated with Zn^{2+} pyrithione. Zn^{2+} pyrithione radiolabeled with ^{65}Zn crosses the plasma membrane (Fig. S5 *C* and *D*) in greater amounts compared with equimolar amounts of added Zn^{2+} alone. In the absence of Zn^{2+} pyrithione, knockdown of ZIP12 reduced neurite length compared with N2a cells (Fig. 3*D*) and differentiated mouse NPCs (Fig. S4*J*) transfected with control shRNA, whereas neurite length was recovered with Zn^{2+} pyrithione treatment. Thus, neurite length could be rescued by increasing intracellular Zn^{2+} availability with Zn^{2+} pyrithione in ZIP12 knockdown cells. Both DTPA and Zn^{2+} pyrithione were used at concentrations that do not affect cell viability (Fig. S5 *E*–*H*). These data indicate that neurite sprouting and length are linked to intracellular Zn^{2+} and ZIP12 expression.

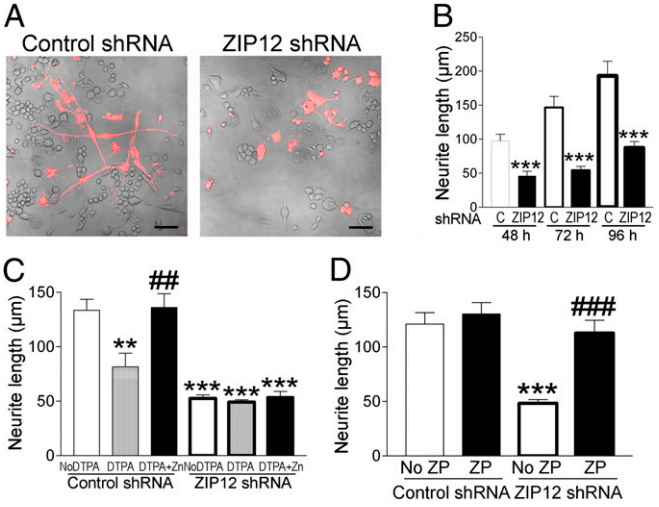

Fig. 3. Neurite extension is dependent on Zn^{2+} transport by ZIP12 and is affected by Zn^{2+} availability. (*A* and *B*) ZIP12 shRNA reduces neurite length in N2a cells ($n = 50$, ± SE). (*C*) Chelation of extracellular Zn^{2+} with DTPA mimics the impairment of ZIP12 knockdown on neurite length in N2a cells ($n = 50$, ± SE). (*D*) Zn^{2+} carrier pyrithione (ZP) restores neurite outgrowth impaired by ZIP12 shRNA knockdown in N2a cells ($n = 50$, ± SE). (Scale bars: 100 μm.) $^{**}P < 0.0$, $^{***}P < 0.001$ versus control cells without DTPA or ZP; $^{\#\#}P < 0.01$, $^{\#\#\#}P < 0.001$ versus control cells with DTPA or ZIP12-shRNA cells without ZP.

ZIP12 Is Important for CREB Signaling and Tubulin Polymerization. We investigated the role of ZIP12 on CREB function because we observed that neurite outgrowth, a CREB signaling-dependent critical step for neuronal differentiation (18), requires ZIP12. N2a cells transfected with ZIP12 shRNA showed reduced CREB activation after differentiation for 48 h (Fig. 4*A*) and impaired phosphorylation at serine 133 (Fig. 4*B*) after incubation in differentiating medium for 30 min at 48 h posttransfection. We did not observe a difference in CREB activation and phosphorylation in undifferentiated cells transfected with control or ZIP12 shRNA. When we differentiated N2a cells while treating them with chelator to eliminate extracellular Zn^{2+} availability (Fig. 4*C*), we observed that DTPA-treated control-shRNA cells showed a reduction in CREB activation that was similar to the reduction induced by ZIP12 shRNA knockdown. This result demonstrates that chelation of extracellular Zn^{2+} eliminates the effect of ZIP12 on CREB activation. CREB phosphorylation was reduced by intracellular Zn^{2+} chelation by TPEN in all conditions tested (Fig. 4*D*), including both undifferentiated and differentiated cells and cells transfected with control or ZIP12 shRNA. These differences in the interactions of Zn^{2+} chelation and ZIP12 expression may be caused by the differing characteristics of the cell impermeant chelator DTPA and the rapid cell permeant chelator TPEN and the time courses of the CREB activation and phosphorylation assays.

We used viral protein 16 (VP16)-CREB, a constitutively active CREB (19), to determine if the effects of Zn^{2+} and ZIP12 on neurite extension could be rescued by CREB activation without the induction of CREB phosphorylation. Transfection of VP16-CREB resulted in an increase in neurite length in N2a cells incubated in control and reduced serum media without RA supplementation after 48 h as compared with cells transfected with control plasmid (Fig. 4*E*). The neurite outgrowth induced by constitutive VP16-CREB activation was not affected by extracellular Zn^{2+} chelation by DTPA (Fig. 4*F*) or by ZIP12 shRNA (Fig. 4*G*). These observations support the concept that CREB activation is Zn^{2+}-dependent and requires ZIP12 expression during neuronal differentiation.

We examined tubulin polymerization states in N2a cells to further our understanding of how neurite length, ZIP12, and intracellular Zn^{2+} might be connected. Knockdown of ZIP12 resulted in a reduction of polymerized tubulin and an increase in soluble tubulin (Fig. 4*H*) compared with the control. Tubulin expression, as measured by α-tubulin in whole-cell extracts, was not affected in either treatment (Fig. 4*H*). The knockdown of ZIP12 did cause an increase in neurite retraction induced by nocodazole, a microtubule-destabilizing agent. Here, neurite length was measured before and after nocodazole treatment for differentiated N2a cells transfected with the control shRNA or the ZIP12 shRNA. Application of 500 nM nocodazole for 30 min resulted in a decrease in neurite length in ZIP12-knockdown cells but not in control cells (Fig. 4*I*). No changes in neurite length were observed when nocodazole was withheld. Reductions in neurite length were evident in both control and ZIP12 shRNA cells when a higher concentration of nocodazole (1.5 μM) was used.

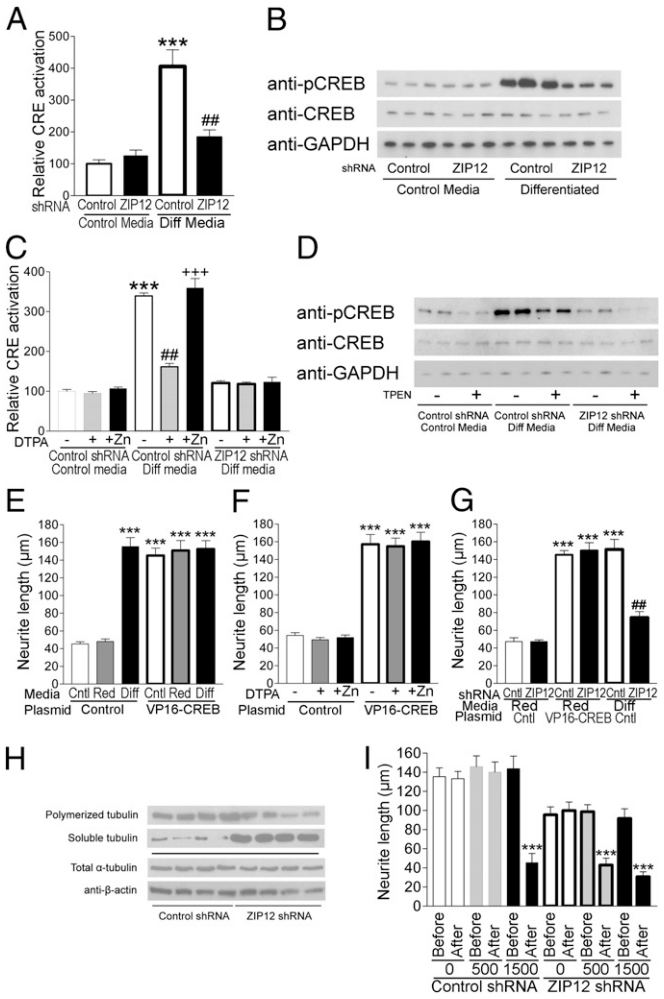

Fig. 4. ZIP12 is required for CREB signaling and tubulin polymerization. (*A* and *B*) Differentiation of N2a cells increases cAMP response element (CRE) activation ($n = 6$, ± SE) and CREB phosphorylation, both of which are blunted by ZIP12 shRNA-mediated knockdown. $^{***}P < 0.001$ versus control undifferentiated cells; $^{\#\#}P < 0.01$ versus control differentiated cells. (*C*) Extracellular Zn^{2+} chelation by DTPA mimics the blunting of CREB activation in differentiated cells induced by ZIP12 shRNA knockdown ($n = 6$, ± SE). $^{***}P < 0.001$ versus control undifferentiated cells; $^{\#\#}P < 0.01$ versus control differentiated cells; $^{+++}P < 0.001$ versus cells treated with DTPA. (*D*) Intracellular Zn^{2+} chelation by TPEN reduces phosphorylation of CREB regardless of ZIP12 shRNA knockdown. (*E*) Constitutive activation of CREB by VP16-CREB1 transfection increases neurite extension in the absence of RA. $^{***}P < 0.001$ versus cells transfected with control plasmid. (*F* and *G*) Neurite outgrowth induced by constitutive activation of CREB is not affected by (*F*) extracellular Zn^{2+} chelation or (*G*) ZIP12 shRNA-mediated knockdown. $^{***}P < 0.001$ versus cells transfected with control plasmid in reduced (Red) serum medium. $^{\#\#\#}P < 0.001$ versus cells transfected with control plasmid and differentiating medium. (*H*) ZIP12 knockdown alters soluble and polymerized tubulin fractions in N2a cells without affecting total tubulin protein expression. (*I*) ZIP12 knockdown in differentiated N2a cells increases sensitivity to neurite retraction following microtubule destabilization by nocodazole ($n = 50$, ± SE). $^{***}P < 0.001$ versus cells before nocodazole.

Differences in tubulin polymerization in N2a cells caused by ZIP12-shRNA knockdown were visible by staining polymerized tubulin with a fluorescent paclitaxel. ZIP12 knockdown resulted in reduced polymerized tubulin in neurites and increased polymerized tubulin staining within the cell body at both 8 h and 48 h differentiation (Fig. S6). Controls displayed staining for polymerized tubulin primarily within neurites. Undifferentiated ZIP12 knockdown cells and control undifferentiated cells displayed no discernible difference in polymerized tubulin content and organization. Polymerized tubulin was visibly prominent in neurites of untransfected cells next to mZIP12-shRNA–transfected cells in the same field of view. Some mZIP12-shRNA–transfected cells showed reduced polymerized tubulin staining in neurites or heavier tubulin staining in the cell body compared with neurites. Collectively, these results link ZIP12-dependent Zn^{2+} transport function to polymerized tubulin within extending neurites.

ZIP12 Is Expressed During Neurulation and Embryonic Nervous System Development in *X. tropicalis*. The *slc39a12* ortholog of *X. tropicalis* shares 52% and 50% of its predicted amino acid sequence with human and mouse ZIP12, respectively, and contains conserved structural features of ZIP proteins. In *X. tropicalis*, *slc39a12* and neighboring genes (contig NW_003163763) share a syntenic relationship with human and mouse, indicating that xZIP12 is the ZIP12 ortholog of this species. Gene expression of xZIP12 in adult *X. tropicalis* was highest in brain tissue, similar to our observations for mouse tissues (Fig. 5*A*). xZIP12 gene expression during development was first detected during early neural plate formation (stage 13) and increased at the early tailbud stage (stage 28). Onset of xZIP12 gene expression seems to be similar to that of N-tubulin (Fig. 5*B*), which first occurs during early neurulation (20). Using quantitative RT-PCR, we observed that xZIP12 mRNA expression is higher in the neural plate than in the rest of the embryo (Fig. 5*C*). In situ hybridization of *X. tropicalis* embryos showed that ZIP12 mRNA expression is highest around the anterior neuropore in the neural plate (Fig. 5*D*), and as embryogenesis proceeds, ZIP12 is present in the forebrain, midbrain, and presumptive eye of the embryo (Fig. 5*D*). These gene-expression patterns suggest that xZIP12 is important during neurulation and subsequent nervous system development.

ZIP12 Is Required for Neurulation and Tubulin Polymerization. Based on the developmental pattern of ZIP12 expression, we investigated the functional role of xZIP12 in neurulation by targeted knockdown with antisense morpholinos (MOs). Morpholino *slc39a12*MO1 prevents the initiation of xZIP12 translation (Fig. S7*A*), whereas morpholino *slc39a12*MO2 causes exon exclusion and premature termination of xZIP12 translation (Fig. S7 *B* and *C*). Embryos injected with *slc39a12*MO1 and *slc39a12*MO2 developed through gastrulation and neural plate formation but delayed at neural tube closure and displayed severe neural tube defects. These defects included incomplete closure of the neural tube (84/100) or developmental arrest after neural tube closure (16/100) for embryos injected with *slc39a12*MO1 (Fig. 5*G*) and delayed closure of the neural tube (45/109) after 22 h for embryos injected with *slc39a12*MO2 (Fig. 5*K*). All embryos injected with *slc39a12*MO1 were dead before developmental stage 22 and all embryos injected with *slc39a12*MO2 were dead before developmental stage 25 (Fig. 5*M*). In contrast, embryos injected with a mismatch morpholino to *slc39a12*MO1 ($n = 41$) were developmentally normal and indistinguishable from embryos injected with control morpholino (Fig. 5 *H* and *I*). Few embryos injected with control morpholino (1/153) (Fig. 5 *F*, *H*, and *J*) showed signs of neural tube defects. Nearly all control-injected embryos (145/153) proceeded through normal development (stages 32–34). Collectively these results support the concept that xZIP12 is required for neurulation during development.

We explored whether xZIP12 affects neurulation through impaired tubulin polymerization. N-tubulin is expressed primarily in the neural tube during closure in *Xenopus laevis* (21), whereas α-tubulin is expressed throughout the embryo. Differences in total N-tubulin and α-tubulin content were not detected in *slc39a12*MO1-injected versus control-injected embryo extracts (Fig. 5*N*). However, a reduced ratio of polymerized to soluble N-tubulin was found in *slc39a12*MO1 compared with control

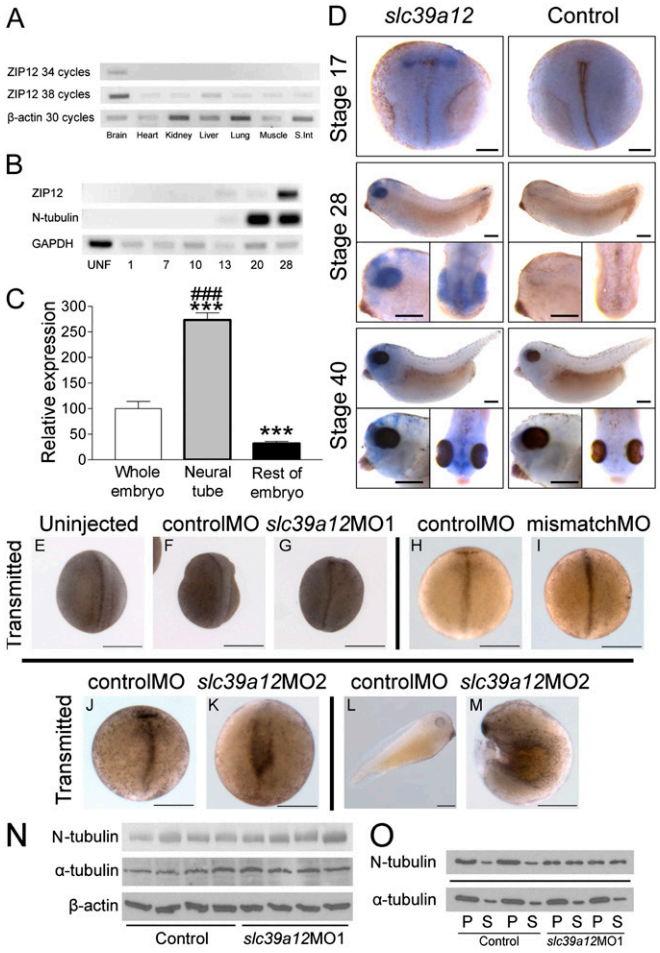

Fig. 5. ZIP12 is expressed primarily in the neural tube and brain of *X. tropicalis* and is required for neural tube closure and embryonic viability. (*A* and *B*) ZIP12 and β-actin or GAPDH expression was determined in various adult tissues and developmental stages by RT-PCR. (*C*) ZIP12 mRNA expression is elevated in the neural plate, as determined by quantitative RT-PCR ($n = 6$, ± SE). ***$P < 0.001$ versus whole embryo; $^{###}P < 0.001$ versus rest of embryo. (*D*) ZIP12 mRNA (*slc39a12*) is expressed during neurulation and early nervous system development, analyzed by in situ hybridization. (*E–M*) ZIP12 knockdown by antisense morpholino microinjection impairs *X. tropicalis* development during neurulation. (*N*) Microinjection of *slc39a12*MO1 does not affect tubulin protein content, analyzed by immunoblotting. (*O*) Microinjection of *slc39a12*MO1 affects the ratio of polymerized to soluble β2-tubulin, as analyzed by polymerized tubulin fractionation and immunoblotting. (Scale bars: 250 μm in all images.)

extracts (Fig. 5*O*). Differences in the ratio of polymerized to soluble α-tubulin were not observed. Taken together, knockdown of xZIP12 impairs normal neurulation and reduces the amount of polymerized *N*-tubulin.

Discussion

Our data show the Zn^{2+} transporter ZIP12 is critical for neuronal differentiation, neurulation, and embryonic development. ZIP12 expression in the brain, conserved across human, mouse, and frog is likely an indicator of evolutionary constraint caused by the requirement of ZIP12 for nervous system development and is consistent with other brain-specific genes (22). The defects in neuronal maturation and neural tube closure caused by ZIP12 inhibition are consistent with the localization and expression of mZIP12 and xZIP12. Zn^{2+} transport by ZIP12 may support an increased demand for Zn^{2+} during early nervous system development (4). Importantly, loss of ZIP12 could not be offset by other numerous Zn^{2+} uptake pathways, such as Zn^{2+}-permeable Ca^{2+} channels (23), or other Zn^{2+} transporters. This finding underscores the importance of ZIP12 in its nonredundant and critical role in neuronal development and neurulation.

The Zn^{2+} uptake activity and cellular distribution of ZIP12 are similar to that of several other members of the SLC39 family. ZIP12-transfected cells have increased Zn^{2+} uptake, a high cellular Zn^{2+} content, and increased cytoplasmic Zn^{2+} concentrations. These changes in cellular Zn^{2+} are similar to those that can be induced by ZIP1, ZIP3, and ZIP4 of the SLC39 family (24), which transit between the plasma membrane and perinuclear regions and transport Zn^{2+} from the extracellular medium. The finding that ZIP12 is detectable at the plasma membrane in primary mouse neurons and transfected CHO cells is supported by proteomic profiling (25), which identified ZIP12 (FLJ30499) by LC-MS using extracted and digested plasma membrane proteins from mouse brain. Similar to the Zn^{2+} transporters ZIP1, ZIP3, and ZIP4 (24), a significant portion of ZIP12 is present away from the plasma membrane, and Zn^{2+} chelation by TPEN results in migration of ZIP12 away from the perinuclear region and toward the plasma membrane. Interplay between the high, nanomolar affinity of ZIP12 for Zn^{2+}, regulation of ZIP12 localization at the plasma membrane, and tissue-specific expression of ZIP12 in the nervous system likely contributes to the role of ZIP12 in development.

Neuronal differentiation requires ZIP12, which links Zn^{2+} to physiological aspects of neuronal development. Previous studies have shown that low dietary Zn^{2+} intake in rats and mice impairs neurite outgrowth in the brain (26, 27). CREB activity and neurite outgrowth are closely linked phases of neuronal differentiation. RA induces rapid CREB phosphorylation, a critical step that controls CREB transcriptional activity and neurite outgrowth (18). Zn^{2+} transport by ZIP12 affects an early stage of neuronal differentiation through CREB phosphorylation, which is evident within 30 min of differentiation. Previous studies have shown Zn^{2+} ionophore PBT2 increases zinc availability, induces CREB phosphorylation, and promotes neuroprotection in cellular models of Alzheimer's disease (28). Furthermore, the role of Zn^{2+} transporters in cell signaling pathways (29–31) has been identified in tissues outside the nervous system. In support of the role of Zn^{2+} in CREB signaling, the constitutive activation of CREB signaling by VP16-CREB, which essentially bypasses the requirement of CREB phosphorylation for activation activity, effectively rescues the impairment in neurite outgrowth caused by either extracellular Zn^{2+} chelation or ZIP12 knockdown. Given the wide range of biological functions for Zn^{2+}, neural differentiation may result in an increased need for Zn^{2+} that is met in part by ZIP12. Although CREB signaling is affected by ZIP12 and Zn^{2+}, it is possible that the impairments in CREB signaling and other factors such as tubulin polymerization reflect a broad delay in differentiation, given the diverse roles of Zn^{2+} in cell metabolism (2). More studies will be needed to determine the roles of ZIP12 and other Zn^{2+} uptake transporters, such as ZIP10 (32), which is highly expressed in both brain and liver, at different stages of neuronal development.

During embryogenesis, knockdown of ZIP12 expression impaired neural tube closure and arrested development. A crucial role of ZIP12 for neurulation is consistent with reports linking dietary Zn^{2+} deficiency in humans to neural tube defects (7). The location of ZIP12 expression and the developmental impairments in ZIP12MO embryos are closely linked. High expression of ZIP12 was detected at the anterior neuropore, the primary site of neural tube closure impairment. ZIP12 expression was concentrated in the eye and head region of *Xenopus* tailbud-stage embryos, and for ZIP12MO embryos that proceeded past neurulation, no optic vesicle or lens development could be

discerned in the presumptive eye region. Tubulin polymerization was impaired in the neural plate of *slc39a12*MO1 morphants. Disruption of microtubules with different agents slows progression of neurulation and impairs neural tube closure in vertebrate embryos (33), similar to the effects seen in ZIP12-knockdown embryos. Chelation of Zn^{2+} in *Xenopus* slows development during neurulation, leading to arrest (34). The correlation between the temporal and spatial expression of ZIP12 and its crucial requirement in neurulation all support the hypothesis that ZIP12 has a specific role in CNS development.

Systematic analyses of tissue-specific patterns of gene coexpression across different species, as proposed by Ala et al. (35), can effectively identify genes critical for nervous system function. McGary et al. (36) have proposed that phenologs, in which disruptions in orthologous genes result in phenotypes across species, can identify candidate disease genes in humans. Further investigation is warranted to determine if ZIP12 is a candidate gene for nervous system defects during prenatal development with increased penetrance during low maternal intake of dietary Zn^{2+}.

Methods

All procedures were approved by the Institutional Animal Care and Use Committee at the University of California, Davis and the Marine Biological Laboratory.

Microinjection of *X. tropicalis* Embryos with Antisense Morpholinos. Embryos were injected at the one-cell stage with 10 ng morpholino with 0.2% rhodamine dextran (Invitrogen) as a tracer.

Additional Methods. Details of microarray data analyses, reagents, cell culture, transfection, Zn^{2+} uptake activity, plasmid construction, luciferase reporter assays, ICP-MS, cell-surface biotinylation, anti-mouse ZIP12 antibody production, indirect immunofluorescence, cell protein isolation, immunoblotting, mouse brain immunohistochemistry, free Zn^{2+} measurements in solutions, Zinpyr-1 staining, flow cytometry, cell viability, RT-PCR, neurite length analyses, in situ hybridization, morpholino sequences and validation, and tubulin organization are described in *SI Methods*. All statistical analyses used are detailed in *SI Methods*.

ACKNOWLEDGMENTS. We thank Maggie Chiu, Carol Oxford, and Joel Commisso for their technical expertise; Jonathan Gitlin and Robert Prendergast for their critical reading of the manuscript; Peter J. S. Smith for his support provided through the Biocurrents Research Center; and Peter Klein for the pCS2+FLAG plasmid (Addgene). We are grateful for the expertise of the National *Xenopus* Resource, funded by National Institutes of Health (NIH) P40 OD010997. This work was supported by the University of California, Davis Center for Health and Nutrition Research (R.B.R.), NIH NCRR Grants P41 RR001395S1 (to Joshua W. Hamilton and M.A.M.) and P30 GM092374 (to Gary G. Borisy), by the Eugene and Millicent Bell Fellowship Fund in Tissue Engineering (M.A.M.), and by the Hermann Foundation Research Development Fund Award (M.A.M.).

1. Song Y, Leonard SW, Traber MG, Ho E (2009) Zinc deficiency affects DNA damage, oxidative stress, antioxidant defenses, and DNA repair in rats. *J Nutr* 139(9):1626–1631.
2. Ho E, Ames BN (2002) Low intracellular zinc induces oxidative DNA damage, disrupts p53, NFkappa B, and AP1 DNA binding, and affects DNA repair in a rat glioma cell line. *Proc Natl Acad Sci USA* 99(26):16770–16775.
3. Frederickson CJ, Koh JY, Bush AI (2005) The neurobiology of zinc in health and disease. *Nat Rev Neurosci* 6(6):449–462.
4. Ames BN (2006) Low micronutrient intake may accelerate the degenerative diseases of aging through allocation of scarce micronutrients by triage. *Proc Natl Acad Sci USA* 103(47):17589–17594.
5. Dufner-Beattie J, et al. (2007) The mouse acrodermatitis enteropathica gene Slc39a4 (Zip4) is essential for early development and heterozygosity causes hypersensitivity to zinc deficiency. *Hum Mol Genet* 16(12):1391–1399.
6. Velie EM, et al. (1999) Maternal supplemental and dietary zinc intake and the occurrence of neural tube defects in California. *Am J Epidemiol* 150(6):605–616.
7. Uriu-Adams JY, Keen CL (2010) Zinc and reproduction: Effects of zinc deficiency on prenatal and early postnatal development. *Birth Defects Res B Dev Reprod Toxicol* 89(4):313–325.
8. Eide DJ (2004) The SLC39 family of metal ion transporters. *Pflugers Arch* 447(5): 796–800.
9. Giunta C, et al. (2008) Spondylocheiro dysplastic form of the Ehlers-Danlos syndrome—an autosomal-recessive entity caused by mutations in the zinc transporter gene SLC39A13. *Am J Hum Genet* 82(6):1290–1305.
10. Fukada T, et al. (2008) The zinc transporter SLC39A13/ZIP13 is required for connective tissue development; its involvement in BMP/TGF-beta signaling pathways. *PLoS ONE* 3(11):e3642.
11. Yamashita S, et al. (2004) Zinc transporter LIVI controls epithelial-mesenchymal transition in zebrafish gastrula organizer. *Nature* 429(6989):298–302.
12. Pielage J, Kippert A, Zhu M, Klämbt C (2004) The Drosophila transmembrane protein Fear-of-intimacy controls glial cell migration. *Dev Biol* 275(1):245–257.
13. Stathakis DG, et al. (1999) The catecholamines up (Catsup) protein of Drosophila melanogaster functions as a negative regulator of tyrosine hydroxylase activity. *Genetics* 153(1):361–382.
14. Dezso Z, et al. (2008) A comprehensive functional analysis of tissue specificity of human gene expression. *BMC Biol* 6:49.
15. Hara H, Aizenman E (2004) A molecular technique for detecting the liberation of intracellular zinc in cultured neurons. *J Neurosci Methods* 137(2):175–180.
16. Tremblay RG, et al. (2010) Differentiation of mouse Neuro 2A cells into dopamine neurons. *J Neurosci Methods* 186(1):60–67.
17. Andersson DA, Gentry C, Moss S, Bevan S (2009) Clioquinol and pyrithione activate TRPA1 by increasing intracellular Zn2+. *Proc Natl Acad Sci USA* 106(20):8374–8379.
18. Cañón E, Cosgaya JM, Scsucova S, Aranda A (2004) Rapid effects of retinoic acid on CREB and ERK phosphorylation in neuronal cells. *Mol Biol Cell* 15(12):5583–5592.
19. Barco A, Alarcon JM, Kandel ER (2002) Expression of constitutively active CREB protein facilitates the late phase of long-term potentiation by enhancing synaptic capture. *Cell* 108(5):689–703.
20. Richter K, Grunz H, Dawid IB (1988) Gene expression in the embryonic nervous system of Xenopus laevis. *Proc Natl Acad Sci USA* 85(21):8086–8090.
21. Moody SA, Miller V, Spanos A, Frankfurter A (1996) Developmental expression of a neuron-specific beta-tubulin in frog (Xenopus laevis): A marker for growing axons during the embryonic period. *J Comp Neurol* 364(2):219–230.
22. Khaitovich P, et al. (2005) Parallel patterns of evolution in the genomes and transcriptomes of humans and chimpanzees. *Science* 309(5742):1850–1854.
23. Sensi SL, et al. (1997) Measurement of intracellular free zinc in living cortical neurons: Routes of entry. *J Neurosci* 17(24):9554–9564.
24. Wang F, et al. (2004) Zinc-stimulated endocytosis controls activity of the mouse ZIP1 and ZIP3 zinc uptake transporters. *J Biol Chem* 279(23):24631–24639.
25. Nielsen PA, et al. (2005) Proteomic mapping of brain plasma membrane proteins. *Mol Cell Proteomics* 4(4):402–408.
26. Dvergsten CL, Fosmire GJ, Ollerich DA, Sandstead HH (1984) Alterations in the postnatal development of the cerebellar cortex due to zinc deficiency. II. Impaired maturation of Purkinje cells. *Brain Res* 318(1):11–20.
27. Gao HL, et al. (2009) Zinc deficiency reduces neurogenesis accompanied by neuronal apoptosis through caspase-dependent and -independent signaling pathways. *Neurotox Res* 16(4):416–425.
28. Crouch PJ, et al. (2011) The Alzheimer's therapeutic PBT2 promotes amyloid-β degradation and GSK3 phosphorylation via a metal chaperone activity. *J Neurochem* 119(1):220–230.
29. Haase H, Rink L (2009) Functional significance of zinc-related signaling pathways in immune cells. *Annu Rev Nutr* 29:133–152.
30. Aydemir TB, Sitren HS, Cousins RJ (2012) The zinc transporter Zip14 influences c-Met phosphorylation and hepatocyte proliferation during liver regeneration in mice. *Gastroenterology* 142(7):1536–1546.
31. Beker Aydemir T, et al. (2012) Zinc transporter ZIP14 functions in hepatic zinc, iron and glucose homeostasis during the innate immune response (endotoxemia). *PLoS ONE* 7(10):e48679.
32. Lichten LA, Ryu MS, Guo L, Embury J, Cousins RJ (2011) MTF-1-mediated repression of the zinc transporter Zip10 is alleviated by zinc restriction. *PLoS ONE* 6(6):e21526.
33. Smedley MJ, Stanisstreet M (1986) Calcium and neurulation in mammalian embryos. II. Effects of cytoskeletal inhibitors and calcium antagonists on the neural folds of rat embryos. *J Embryol Exp Morphol* 93:167–178.
34. Jörnvall H, Falchuk KH, Geraci G, Vallee BL (1994) 1,10-Phenanthroline and Xenopus laevis teratology. *Biochem Biophys Res Commun* 200(3):1398–1406.
35. Ala U, et al. (2008) Prediction of human disease genes by human-mouse conserved coexpression analysis. *PLOS Comput Biol* 4(3):e1000043.
36. McGary KL, et al. (2010) Systematic discovery of nonobvious human disease models through orthologous phenotypes. *Proc Natl Acad Sci USA* 107(14):6544–6549.